



EFFECT OF PIN VOLUME RATIO ON MICROSTRUCTURAL CHARACTERISTICS OF FRICTION STIR PROCESSED ALUMINIUM BASED METAL MATRIX COMPOSITE

¹Vijayavel P* and ²Balasubramanian V

¹Research Scholar, Centre for Materials Joining and Research (CEMAJOR), Department of Manufacturing Engineering, Annamalai University, Annamalai Nagar - 608 002, Tamil Nadu, India.

²Centre for Materials Joining and Research (CEMAJOR), Department of Manufacturing Engineering, Annamalai University, Annamalai Nagar - 608 002, Tamil Nadu, India.

ABSTRACT

FSW was invented at the welding institute (TWI) of the United Kingdom in 1991 as a solid-state joining technique and was initially applied to aluminium alloys. Friction Stir Processing (FSP) is an adaptation of friction stir welding with the following unique features. Low amount of heat generation, extensive plastic flow of material, very fine grain size in the stirred zone, healing of flaws and casting porosity, random misorientation of grain boundaries in the stirred region, mechanical mixing of the surface and subsurface layers, Therefore, the FSP can be used as a generic process to modify the microstructure and change the composition, at selective location. In FSP, the effect of pin profile on material flow, material mixing, material consolidation is predominant than other parameters. Hence, in this work, the effect of pin volume ratio (dynamic volume/static volume) on microstructural characteristics of aluminium based metal matrix composites was characterized. Microhardness of FSP region was measured and correlated with respective microstructural characteristics. From this investigation it is found that pin volume ratio of 1.15 exhibited defect free stir zone with higher hardness compared to other ratios. The reasons for the above effects are discussed in detail in this paper.

Key words: Friction Stir Processing; Pin Volume Ratio; Microstructure

1. Introduction

Stir casted aluminum (Al) based metal matrix composites (MMCs) have the beneficial properties of both metals and ceramics like good corrosion resistance, low electrical resistance and excellent mechanical properties [1,2]. Silicon carbide particulate (SiCp) reinforced Al-alloy composites are now being exploited commercially thanks to the technological advancing in their applications such as aerospace, sports items, transportation and ship building etc [3]. Despite of its beneficial properties, the quality of the composite materials was inherently affected by the fabrication process itself. The composite materials are suffered from porosity, uneven distribution of reinforcement particles etc. which have an effect on the services of the composite materials. These composites also suffered from low ductility and toughness due to incorporation of the uneven distribution of hard ceramic reinforcement.

The quality fabrication of composite materials were limited due to the difficulty in achieving a uniform

distribution of the reinforcement material, mutability between the two main substance, porosities in the cast metal matrix composites, chemical reaction between reinforcement material and the matrix alloy [4,5].

Surface modification techniques can improve the grain size of the MMCs by altering the above – mentioned properties, one such technique is attempted in the present work, known as friction stir processing (FSP). FSP is an offshoot of friction stir welding (FSW) which is a solid state welding technique patented by The Welding institute of Institute of United Kingdom in 1991 [6]. FSP technique has been used to produce surface composites on aluminium substrates [7]. In this technology, a rotating tool, with specially designed tool profiles and shoulder is inserted into a substrate material tool and produces a recrystallized fine grained micro structure within the stirred zone (SZ). This process was explained in detail elsewhere [8].

Hsu et al. [10] achieved ultrafine grained Al-Al₂ Cu composite by FSP, which has high Young's modulus, good compressive strength and ductility.

*Corresponding Author - *Email: vijayavelfsp@gmail.com.

Sentella et al [11] studied the effect of FSP on the mechanical properties of cast A356 and 319A1 alloys and observed that the cast uneven grains structure was replaced with fine equiaxed structure in the stir zone.

FSPed alloys improved the tensile strength, ductility and fatigue strength. FSP was successfully employed to fabricate AZ63 magnesium alloy and SiC bulk composites. The nanoSiC particles effected significant improvement in the tensile strength and hardness in the bulk composite against the as cast samples [12]. Friction Stir processing of light aluminium, magnesium and titanium alloys were studied by may researchers and proved that FSP resulted in breaking up of coarse dendrites and secondary phases [13].

The tool pin profile plays a dominant role in the formation of the stir zone regions [14]. Elangovan et al., [15] investigated the characteristics of friction stir welded aluminium alloys in relation with the dynamic and static volume ratio generated by various tool pin profiles. Through many investigations have been carried out to understand the effect of pin profile on friction stir welding of aluminium alloys, very few investigations have been reported so foron FSP of Al based MMCs. Moreover, the effect of tool pin profile in tapers of pin volume ratio (dynamic volume / static volume) has not get investigated on FSP of Al based MMCs. Hence, in this investigation, an attempt has been made to analyze the effect of the pin volume ratio on stir zone characteristics and the results are presented in this paper.

2. Experimental Work

2.1 Material preparation

In this study, the work piece material LM25 Aluminum based metal matrix composites with the reinforcement of SiC particles with 5% volume percentage was prepared via stir casting route and they were machined to rectangular plates of size 200 X 100 X 12 mm.

Table 1. Chemical composition (wt %) of base material

	Si	Mg	Fe	Mn	Cu	Ti	Ni	Zn	SiC	Al
LM25AA-SiCp MMC	7.5	0.6	0.5	0.3	0.2	0.2	0.1	0.1	5%	Balance

The chemical composition of MMC and the mechanical properties of MMCs used in this investigation are presented in Table 1 and Table 2 respectively.

Table 2. Mechanical properties of the base material (LM25 AA-SiCp)

Yield strength (MPa)	Ultimate tensile strength (MPa)	Elongation (%)	Reduction in cross sectional area (%)	Micro hardness @ 0.49 N (HV)
143	155	2	4.5	68

2.2 Fabrication of tools with different pin profiles

Four FSP tools with different tool pin profiles (straight cylindrical (STC), threaded cylindrical (THC), Tapered cylindrical (TAC), threaded tapered cylindrical (TTC)) were fabricated from super high speed steel rod.

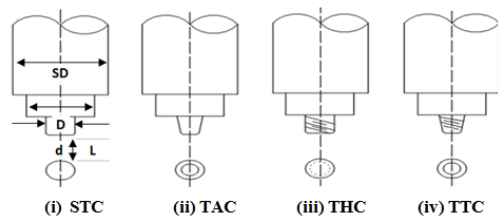


Fig. 1 Schematic of tool pin profiles

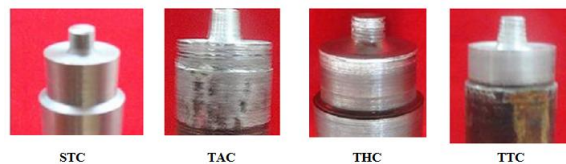


Fig. 2 Profiles and photographs of Tools used in this investigation

Table 3. Tool Dimensions

(i)	Shank diameter, SD (mm)	26
(ii)	Shoulder diameter, D (mm)	21
(iii)	Pin diameter, d (mm) in STC and THC	7.2
(iv)	Taper Angle, θ (deg) in TAC and TTC	6.73
(v)	Pin length, L (mm)	7.2
(vi)	Pitch (mm) in THC and TTC	1.2






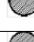
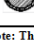
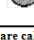
All the tools were machined and flame hardened to improve the tool hardness. The dimensions of the tools are presented in Table 3. The different pin profiles are schematically shown in Fig. 1.

The profiles and photograph of tools used in this investigation are displayed in Fig. 2. The tool dimensions are specified in Table 3.

2.3 Calculation of pin volume ratio (PVR)

The pin generally has cylindrical plain, frustum tapered, threaded and flat surfaces. Pin profiles, other than straight cylindrical are associated with eccentricity. This eccentricity allows incompressible material to pass around the pin profile. Eccentricity of the rotating object is related to dynamic orbit due to eccentricity [16]. This dynamic orbit is a part of the FSW process and different pin profiles exhibit different dynamic orbits. The relationship between the static volume and dynamic volume decides the path for the flow of plasticized material from the leading edge to the trailing edge of the rotating tool. The calculated tool volume ratio is equal to 1.0 for straight cylindrical (STC), 1.15 for tapered cylindrical (TAC), 1.28 for threaded cylindrical (THC) and 1.63 for threaded tapered cylindrical (TTC) pin profiles. These details are shown in Table 4.

Table 4. Ratio between Dynamic Volume to Static Volume of Tool Pin Profiles

Type of Tool	Area occupied by the pin in static condition (mm ²)	Static Volume, V _s (mm ³)	Area occupied by the pin in dynamic condition (mm ²)	Dynamic Volume, V _d (mm ³)	Dynamic/Static Volume (V _d /V _s)
STC		293.14		293.14	1
TAC		253.85		293.14	1.15
THC		229.38		293.14	1.28
TTC		179.62		293.14	1.63

Note: The static and dynamic volumes are calculated for the pin height of 7.2 mm

2.4 Friction stir processing

Friction stir processing was done on the rectangular plates by securing the plates in position using mechanical clamps. A non-consumable tool made of super high speed steel was used in the process. An indigenously designed and developed computer numerically controlled (CNC) FSW machine (22KW: 4000 r/min:6 ton) was used to friction stir processing (FSP). The microstructure and the properties of the friction stir processed surface are generally influenced by the major parameters such as tool rotational speed, tool traverse speed, tool shoulder to pin diameter (D/d) ratio, axial force, pin or probe length, tool pin profiles, etc. In this investigation, several trial runs were conducted by varying the values of these process parameters. Here, the tool pin profile was given prime importance in order to understand the changes effected by various tool pin profiles on microstructure and microhardness of the friction stir processed surface. The parameters used to conduct FSP are presented in Table 5.

Table 5. FSP Parameters

Process Parameters	Unit	Values
Tool rotational speed	rpm	1000
Tool traverse speed	mm/min	40
Axial force	kN	3

Longitudinal microstructure test specimens were extraction of from the friction stir processed zone and the schematic of the extracted specimen is shown in Fig.3. All other parameters except the tool pin profile were kept constant in order to study the effect of the tool pin profile alone.

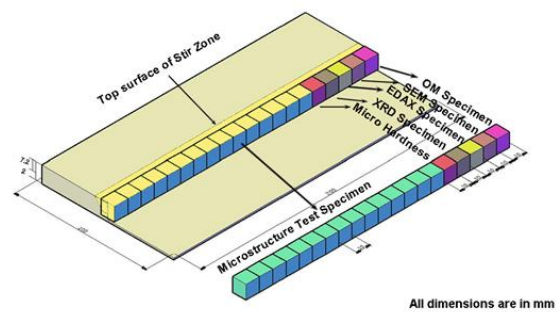


Fig. 3 Scheme of extraction of characterization specimen

3. Results and Discussion

3.1 Effect of pin volume ratio on stir zone area

Friction stir processed surfaces are prone to certain other defects like kissing bond, pinhole, cracks, tunnel defects etc. The eccentricity of the tool pin profile facilitates the movement of the incompressible material around the tool pin. Thomas WM et al., [16], which are caused by the improper flow and insufficient consolidation of the material in the stirred region. The images of the top surface of the as FSPed material were captured using a low magnification digital scanner and presented in Table 6.

The cross-section of the FSPed material was prepared following the standard metallographic procedures and then the images were captured using stereo zoom microscope at 5X magnification. Modest vertical flow and material extrusion from front to back around both sides of the pin is possible and the role of the rotating pin is to provide frictional heating to make the extrusion possible. Ying et al., [17], visualized the solid state material flow in the FSW of AA2024 and AA6013 aluminium alloys reported that the flow of the plate material on the advancing side and the retreating side were different. The macrographs are displayed in Table 6.

Table 6. Macrographs of FSPed region



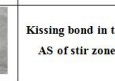


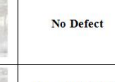


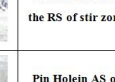

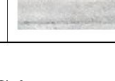
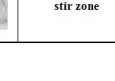

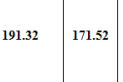

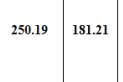

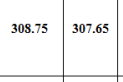

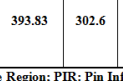
PVR	Tool pin profile	Cross section		Top surface	Observation
		AS	RS		
1.0	Straight Cylindrical (STC)				Kissing bond in the AS of stir zone
1.15	Tapered Cylindrical (TAC)				No Defect
1.28	Threaded Cylindrical (THC)				Tunnel defect in the RS of stir zone
1.63	Threaded Tapered Cylindrical (TTC)				Pin Hole in AS of stir zone

Table 7. Measured Stir zone areas

PVR	Pin Profile	Macrograph		Area of SIR (mm ²)	Area of MIR (mm ²)	Area of PIR (mm ²)	Total Area of Stir zone (mm ²)
		AS	RS				
1.0	Straight Cylindrical (STC)			191.32	171.52	198.12	560.86
1.15	Tapered Cylindrical (TAC)			250.19	181.21	215.28	646.68
1.28	Threaded Cylindrical (THC)			308.75	307.65	216.96	833.36
1.63	Threaded Tapered Cylindrical (TTC)			393.83	302.6	180.04	876.43

SIR: Shoulder Influenced Region; MIR: Middle Region; PIR: Pin Influenced Region

From the macrostructure analysis, it could be inferred that the stir zone produced by the straight cylindrical, threaded cylindrical and threaded tapered cylindrical pin profiles consist of one or other defects. However, the stir zone processed with tapered cylindrical pin profile is free from defects. The cross sections of the FSPed stir zones were partitioned into top, middle and bottom regions along the length of the tool pin as shown in Table 7. The top region is influenced by the tool shoulder and hence referred as Shoulder Influenced Region (SIR) and the bottom region is influenced by the tool pin, hence referred as Pin Influenced Region (PIR). This way of analysis would help to understand the role of the tool shoulder and pin in generating the friction stir processed zone. This perspective also enables to calculate the area generated by the tool shoulder and the pin separately. Breaking up the total stir zone area into three different zones would also help to identify the mechanism behind the defect formation.

It could be inferred from the results that the threaded cylindrical (THC) pin profile exhibited highest stir zone area when compared to the other tool pin profiles. The large stir zone area indicated more material displacement and less consolidation. The threads present in the pin facilitated increased material displacement. This could be reconfirmed by the high SIR and MIR values exhibited by this pin profile which was indication of excessive material displacement, especially at the upper half of the stir zone. The geometry of this pin profile facilitated much material displacement on the advancing side, however all the material on advancing side was not transported to the retreating side. This caused tunnel defect on the retreating side deteriorating the mechanical properties.

TTC pin managed to transport some of the displaced material down by the virtue of its taper feature. However, the insufficient material availability at the advanced side of the bottom region (PIR) produced a pin hole defect on the AS of stir zone. This is evident from the least value of PIR. The stir zone resembled an inverted bell shape with a wider SIR. TAC pin produced a moderate stir zone area and tool volume ratio. From the results, it was observed that the tool volume ratio 1.15 produced better properties, hence could be considered optimal.

The data points presented in Table 7 are connected by the best fit line as shown in Fig. 4. From the graph, it is understood that the stir zone area increases with the increase pin volume ratio. There is a linear direct proportionality between pin volume ratio and stir zone area. The regression equation governing this best fit line is given below:

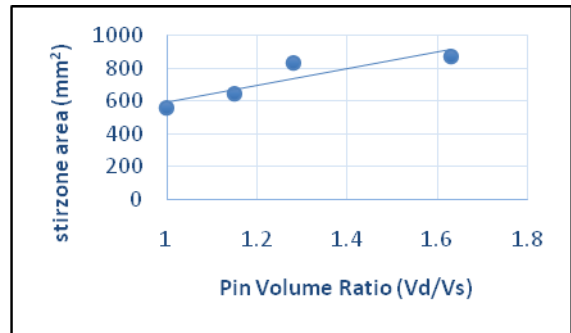


Fig. 4 Effect of Pin volume ratio on stir zone area

$$TAS = [504.39 (Vd/Vs) + 91.285] \text{ mm}^2 \text{ ----- (Eqn 1)}$$

The total area of the stir zone (TAS) can be estimated for a known (Vd/Vs) ratio using the above relationship.

3.2 Effect of pin volume ratio on stir zone microstructure

The specimens for microstructure analysis were cut perpendicular to the FSPed direction using an wire-cut electrical discharge machine. All the processed stir zones of the samples were polished using a grit sequence of 500, 1000, 1200, 2000, 2500 and 3000. After polishing, proper etching was done using the modified Keller’s reagent of 5 ml of HCl, 5 ml of HF, 2 ml of HNO₃ and 19 ml of distilled water were used to reveal the microstructure. Microstructures of stir zones for four different tool pin profiles are displayed in Figs.5 and 6. Fig. 5 displays the light optical micrographs of the stir zone microstructure and Fig. 6 provides the scanning electron micrographs of the stir zones for a more detailed analysis.

Further, an attempt was made to measure the average grain size and average SiCp size in the stir zone as per the ASTM: 112 guidelines and the results are presented in Table 8.

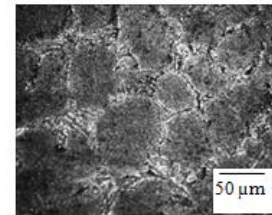
It is evident from the microstructures that the coarse aluminium dendrites and the SiC particles present in the cast aluminium (base material) were broken down by friction stir processing and distributed uniformly in the matrix.

Table 8. Effect of PVR on average grain size and SiCp size

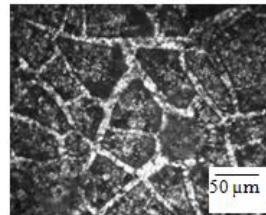
Tool Profile	PVR	Average grain size of the matrix (µm)	Average SiCp Size (µm)
STC	1.0	25	18
TAC	1.15	20	10
THC	1.25	30	14
TTC	1.63	35	18

The stir zone is characterized by relatively fine recrystallized grains and evenly distributed SiC particle in the Al Matrix. The stirring action of the tool causes intense plastic deformation and in situ extrusion of aluminum alloys, Palanivel et al., [18].

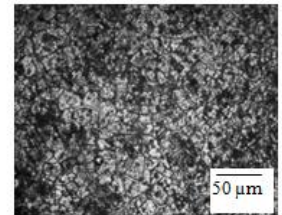
Microstructures of processed zone for four different tool pin profiles are displayed in Fig. 5 and Fig. 6. It could be inferred from the microstructures that the taper cylindrical pin produced finer equiaxed grains and uniformly distributed fine SiC particles when compared to others. These fine grains and particles were



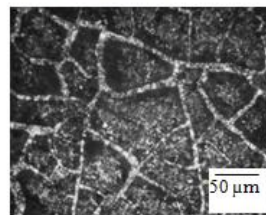
(a) Base material



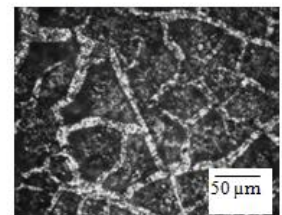
(b) PVR=1.00 (STC)



(c) PVR=1.15 (TAC)



(d) PVR=1.28 (THC)



(e) PVR=1.63 (TTC)

Fig. 5 Effect of pin volume ratio (PVR) on stir zone microstructure (Optical micrograph)

effectively mobilized by the tool pin, causing a smooth material flow and consolidation producing defect free surfaces. The taper threaded cylindrical pin profile with the highest tool volume ratio produced coarser grains and particles. It is inferred from Fig.7 that the particle size decreased with an increase in tool volume ratio and then increased. Very fine equiaxed grains were produced due to dynamic recrystallization and the particles were distributed uniformly throughout the stir zone at the optimum tool volume ratio of 1.15. TAC tool pin profile displaced the right volume of the material, generated enough amount of heat to recrystallize the grains and produced the mechanical work to break up the SiC particles.

The average grain size (AGS) can be estimated for a known (Vd/Vs) ratio using the empirical relation,
 $AGS = [19.825 (Vd/Vs) + 2.4216] \mu m$ --- (Eqn 2)

Similarly, the average SiCp size (ASP) can be estimated for a known (Vd/Vs) ratio using the empirical relation, Similarly, the average SiCp size (ASP) can be estimated for a known (Vd/Vs) ratio using the empirical relation,

$$ASP = [3.965(Vd/Vs) + 9.9843] \mu m \dots\dots\dots (Eqn 3)$$

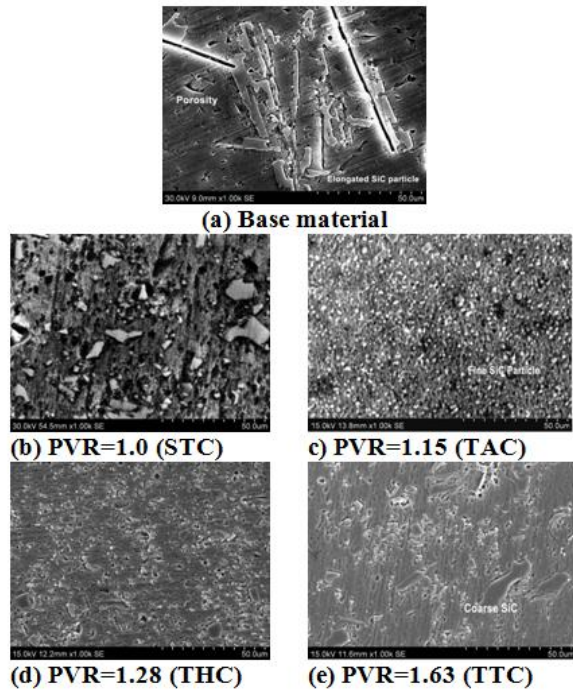


Fig. 6 Effect of pin volume ratio (PVR) on stir zone microstructure (Scanning Electron Micrograph)

3.3 Effect of pin volume ratio on stir zone microhardness

Microhardness was measured extensively in the stir zone using Vickers Microhardness tester (Make:Shimadzu: Japan, Model: Model: HMV-2T) with a load of 49 N and a dwell time of 15 s. As mentioned earlier, the microhardness was measured in all the three regions of stir zone (SIR, MIR and PIR). In each region, 10 readings were taken and the average of 10 readings are presented in Table 9. Though the material influenced by tool shoulder (SIR) alone will control the friction and wear behavior of the FSPed material, the hardness was measured along the thickness direction to understand the homogeneity of FSP region. The average hardness of the base material, LM25AA-5% SiCp metal matrix composite was found to be 68 HV. Higher hardness of the aluminium composites is associated with the size and distribution of the grains and SiC particles according to the Hall-Petch relationship. The segregation of SiC particles along the grain boundaries result in grain boundary pinning causing high dislocation density, which in turn results in higher hardness. The refinement of both the SiC particles and grains also contributed to the increase in the hardness of the stir zone [19,20]. All friction stir processed zones exhibited higher hardness when compared to the base material due to grain refinement. Homogeneous dispersion of the reinforcement in Aluminium matrix

plays an important role [21]. It could be inferred from the results that the tapered cylindrical pin produced the finest grains and particles, which were uniformly distributed as well.

Table 9. Average Microhardness of various regions of friction stir processed material

Tool Pin Profile	PVR	Average hardness of SIR (HV0.05)	Average hardness of MIR (HV)	Average hardness of PIR (HV)
STC	1.0	90	80	73
TAC	1.15	130	120	104
THC	1.28	98	88	81
TTC	1.63	96	86	70

From the macrostructure, we understand that the plain taper cylindrical pin profile generated a well-defined, uniformly shaped stir zone when compared to others. In other words, the areas of the shoulder influenced region (SIR), middle region (MIR) and the pin influenced region (PIR) have closely related values maintaining a uniform stir zone. The area of the shoulder influenced region (SIR) of the plain taper cylindrical pin profile was neither too large (as in THC, TTC) nor too small as in SC, but an optimal one producing good consolidation. This optimal area and consolidation effected by the shoulder and the major taper area of the pin just beneath the shoulder increased the micro hardness value. However, the surfaces processed with other tool pin profiles exhibited lower micro hardness due to the defects present in the stir zone area.

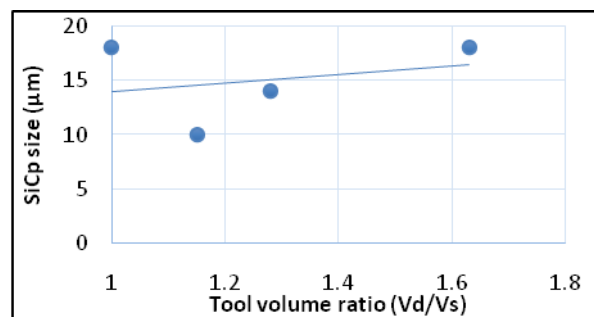


Fig. 8 Effect of pin volume (PVR) ratios on average SiCp size

The SC and THC pin processed stir zones had tunnel defect indicating insufficient material flow and consolidation. However, the TTC pin processed stir zone exhibited pin hole defect due to excessive turbulent movement of the displaced material. This could be compared with the highest tool volume ratio produced the TTC pin profile. TTC pin displaced excess material due to the additional features of thread and taper.

However, it failed to produce enough consolidation of the displaced material. Moreover, the wider SIR of the TTC pin profile clearly indicates that the material was not given enough consolidation. This is evident from the area of the stir zone regions. Hence, this pin profile was not able to produce the hardness as high as TAC pin profile.

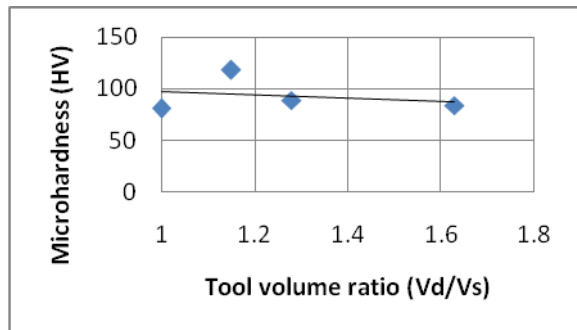


Fig. 9 Pin volume ratio (PVR) on average Microhardness of FSPed material

The average measured hardness of shoulder influenced region (SIR) of FSPed material, presented in Table 9 are fitted by a straight line as shown in Fig 8. From Fig 8 it can be inferred that the micro hardness shows a decreasing trend with increasing tool volume ratio. The micro hardness of the FSPed zone (SHZ) can be estimated for a known (Vd/Vs) ratio using the following relationship (governing equation for the best fit line shown in Fig. 9)

$$\text{SZH} = [-14.016 (\text{Vd/Vs}) + 110.73] \text{HV} \quad \text{----} \quad (\text{Eqn 4.})$$

4. Conclusions

An attempt was made in this investigation to study the effect of different tool pin profiles in terms of pin volume ratio on the stir zone area, microstructure, and micro hardness. The following important conclusions are derived as a result of this investigation

1. The pin volume ratio (PVR) plays a vital role in the formation of stir zone microstructure, reinforcement size and distribution and subsequently controls the hardness of the FSPed material.
2. The stir zone area, average grain size and average particle size are found to be directly proportional to pin volume ratio.
3. Of the four pin profiles investigated in this study, tapered cylindrical (TAC) pin with a PVR of 1.15 yielded defect free friction stir processed zone with finer grains, uniformly distributed reinforcement particles and higher hardness.

4. The size of SiCp decreases in the beginning upto the PVR of 1.3 and then starts to increase with increasing PVR.

Acknowledgement

The first author wish to place his sincere thanks to University Grants Commission (UGC) for financial support provided under the scheme of Rajiv Gandhi National Fellowship (RGNF).

References

1. Pardo A Merino M C Merino S Viejob F carbonerasa M and Arrbal R (2005), "Influence of reinforcement Proportion and matrix composition on pitting corrosion behavior of cast aluminium matrix composites (A3XXX/SiCp)", *Corrosion sciences*. Vol. 451,750-64.
2. Puviyarasan M and Praveen C (2011), "Fabrication and analysis of bulk scip reinforced aluminum metal matrix composites using friction stir process", *World Academy of Sciences Engineering and Technology*, Vol.58, 884-88.
3. Mirchse (1991), *scripta material*, Vol. 1:25.
4. Buffa G Fratini L Pastas and Shivpuri R (2008), "On the thermo- mechanical loads and the resultant residual stresses in friction stir processing operations", *CIRP Ann Manu Tech*, Vol.57, 287-90.
5. Santeella M I Engstrom T storjohann D and Paniy (2003), "Effect of friction stir processing on mechanical properties of the cast aluminum alloy A319 and A356", *Scripta Material*, Vol. 53, 201-06.
6. Thomas W M Nicholas E D Needha J S Murch M G Templesmith P and Dawes C S (1991), "Friction stir butt welding", *International Patent Application NO. PCT/GB92/9125978.8.1991*.
7. Mishara R S Ma Z Y and charit I (2002), "Friction stir processing a novel technique for fabrication of surface composites material", *Material Science Engineering A*, Vol. 341, 307-10.
8. Elangovan K and Balasubramanian V (2007), "Influence of pin profile and rotation speed of the tool on the formation of friction stir processing zone in AA2219 aluminium alloy", *Materials Science Engineering A*, Vol.459, 7-18.
9. Spowart J E Ma Z Y Mishra R S Jata K V Mahoney M W Mishra R S Semiatin S L and Lienert T (2003), "Friction stir welding and processing II", *TMS*, Vol. II, 243-52.
10. Hsu C J Kao P W and Ho N J (2005), "Ultrafine-grained Al-Al2Cu composite produced in situ by friction stir processing", *Scepter Material*, Vol.53, 341-45.
11. Senteella M L Engstrom T Storjohann D and Pan I Y (2005), "Effects of friction stir processing on mechanical properties of the cast aluminum alloy A319 and A356", *Scripta Materialia*, Vol.53, 201-06.
12. Sun K Shi Q Y Sun Y J and Chen G Q (2012), "Microstructure and mechanical property of nano-SiCp reinforced high strength Mg bulk composites produced by Friction stir processing", *Material Science Engineering A*, Vol. 547, 32-34.

13. Ma Z Y Pilchak A L Juhas M S and Williams C (2008), "Microstructural refinement and property enhancement of cast light alloys via friction stir processing", *Scripta Materialia*, Vol. 58, 361-66.
14. Sato Y S Kokawa H Enmoto M and Jogan S (1999), "Microstructural evolution of 6063 aluminum during friction stir welding", *Metall Mater Trans A*, Vol. 30, 2429-37.
15. Elangovan K and Balasubramanian V (2008), "Influences of tool pin profile and tool shoulder diameter on the formation of friction stir processing zone in A6061 aluminium alloy", *Materials and Design*. Vol. 29, 362-73.
16. Thomas W M and Nicholas E D (1997), "Friction stir welding for the transportation industries", *Mater Des*. Vol. 18, 269-73.
17. Ying Li Murr L E and McClure J C (1999), "Solid state flow visualization in the Friction stir welding of 2024Al to 6061Al", *Scripta Mater*, Vol. 40(9), 1041-46.
18. Palanivel R Koshy Mathews P Murugan N and Dinaharan I (2012), "Effect of tool rotational speed and pin profile on microstructure and tensile strength of dissimilar friction stir welded AA5083-H111 and AA6351-T6 aluminum alloys", *Materials and Design*, Vol.40, 7-16.
19. Feng A H Xiao B L and Ma Z Y (2008), "Effect of Microstructural evolution on mechanical properties of friction stir welded AA2009/SiCp composite", *Composites Science Technology*, Vol. 68, 2141-48.
20. Akramifard H R Shamanian M Sabbaghian M and Esmailzadadeh M (2014), "Microstructure and mechanical properties of Cu/SiC metal matrix composites fabricated via friction stir processing", *Mater and Design*, Vol. 54, 838-44.
21. Jeyasimman Sivaprasad Senthilkumar and Narayanasamy (2013), "Carbon nanotube reinforced aluminium alloy composites- A review", *Journal of Manufacturing Engineering*, Vol. 8, Issue. 2, 75-84.